

Cite this article as: Bechsgaard T, Lindskow T, Lading T, Røpcke DM, Nygaard H, Johansen P *et al.* Biomechanical characterization and comparison of different aortic root surgical techniques. *Interact CardioVasc Thorac Surg* 2018; doi:10.1093/icvts/ivy187.

## Biomechanical characterization and comparison of different aortic root surgical techniques

Tommy Bechsgaard<sup>a,b,c</sup>, Thomas Lindskow<sup>b,c</sup>, Troels Lading<sup>b,c</sup>, Diana M. Røpcke<sup>b,c</sup>, Hans Nygaard<sup>b,c</sup>, Peter Johansen<sup>a,b,c</sup>, Sten L. Nielsen<sup>b,c</sup> and J. Michael Hasenkam<sup>b,c,\*</sup>

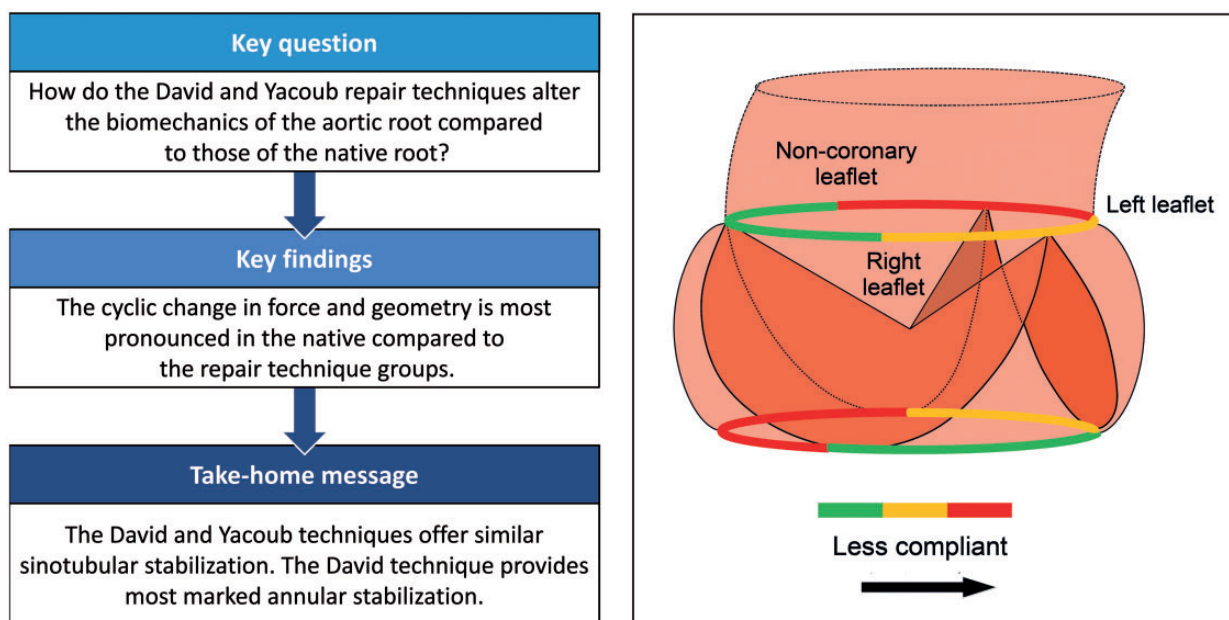
<sup>a</sup> Department of Engineering, Faculty of Science and Technology, Aarhus University, Aarhus N, Denmark

<sup>b</sup> Department of Cardiothoracic & Vascular Surgery, Aarhus University Hospital, Aarhus N, Denmark

<sup>c</sup> Department of Clinical Medicine, Aarhus University Hospital, Aarhus N, Denmark

\* Corresponding author. Department of Cardiothoracic & Vascular Surgery, Aarhus University Hospital, Palle Juul-Jensens Boulevard 99, 8200 Aarhus N, Denmark. Tel: +45-7845-3089; fax: +45-7845 3079; e-mail: hasenkam@clin.au.dk (J.M. Hasenkam).

Received 17 December 2017; received in revised form 22 April 2018; accepted 12 May 2018



### Abstract

**OBJECTIVES:** Understanding the biomechanical impact of aortic valve-sparing techniques is important in an era in which surgical techniques are developing and are increasingly being used based on biomechanical understanding that is essential in the refining of existing techniques. The objective of this study was to describe how the valve-sparing remodelling (Yacoub) and reimplantation (David Type-1) techniques affect the biomechanics of the native aortic root in terms of force distribution and geometrical changes.

**METHODS:** Two force transducers were implanted into 22 pigs, randomized to 1 of 3 groups (David = 7, native = 7 and Yacoub = 8) along with 11 sonomicrometry crystals and 2 pressure catheters. Force and geometry data were combined to obtain the local structural stiffness in different segments of the aortic root.

**RESULTS:** The radial structural stiffness was not different between groups ( $P = 0.064$ ) at the annular level; however, the David technique seemed to stabilize the aortic annulus more than the Yacoub technique. In the sinotubular junction, the native group was more compliant ( $P = 0.036$ ) with the right-left coronary segment than the intervention groups. Overall, the native aortic root appeared to be more dynamic at both the annular level and the sinotubular junction than both intervention groups.

**CONCLUSIONS:** In conclusion, the David procedure may stabilize the aortic annulus more than the Yacoub procedure, whereas the leaflet opening area was larger in the latter ( $P=0.030$ ). No difference ( $P=0.309$ ) was found in valve-opening delay between groups. The 2 interventions show similar characteristics at the sinotubular junction, whereas the David technique seemed more restrictive at the annular level than the Yacoub technique.

**Keywords:** Biomechanical characterization • Force measurements • Aortic root repair • Geometrical analysis

## INTRODUCTION

Aortic root pathologies, which include aneurysms and dissection, are often treated surgically with a composite graft [1, 2]. Since the original technique was introduced, several modifications have been proposed and yielded good long-term results [3, 4]. However, several drawbacks are associated with the replacement of the aortic valve with a mechanical heart valve, such as lifelong anticoagulation medication, risk of thromboembolism and mechanical heart valve noise [5, 6]. In the early 1990s, David and Feindel [7] described the reimplantation technique, while Sarsam and Yacoub [8] proposed the remodelling technique. In both procedures, the native aortic valve is preserved and a graft is used to repair the aortic root defect. In the Yacoub procedure, the aortic valve is sutured onto a scalloped graft, which is reported to preserve annulus dynamics along with the sinus of Valsalva. However, it does not address aortic root dilation caused by connective tissue disorders, for example.

In the original David procedure, a straight tubular graft is used in which the aortic valve is reimplanted, thus addressing root dilation. However, in the original procedure, annular dynamics are compromised and the sinuses are removed, which may cause increased stress on the aortic valve apparatus [9].

Since the original procedures were described, several modifications have been proposed [10]. The 3-dimensional structural changes of the aortic root [11–13] have been described in ovine models. However, there is a lack of *in vivo* aortic root force measurements and investigations on how force alterations in parallel lead to geometric changes.

This is important since it may influence both the function of the aortic valve and the durability of the repair. Furthermore, such relationships can help in refining existing procedures and aid in selecting the optimal treatment for each individual patient.

The hypothesis for the present study is that the Yacoub procedure better preserves the aortic root dynamics, whereas the David procedure better stabilizes the structure by reducing the aortic root forces.

The aim of this study was to assess and describe the biomechanical changes in the native aortic root after the original David Type-1 reimplantation or the Yacoub remodelling procedure. More specifically, the aim was to characterize the geometrical changes coupled with the change in force at both the aortic root annulus and the sinotubular junction (STJ).

## MATERIALS AND METHODS

### Experimental protocol

In this acute experimental study, 28 pigs (mixed Duroc and Danish Landrace) with an average bodyweight of 80 kg were included. Handling of the animals was conducted in compliance with Danish law, and the study was approved by the Danish Inspectorate of Animal Experimentation. Upon arrival at the

operating theatre, the pigs were randomized by drawing lots from sealed envelopes into 1 of 3 groups: a native group, a reimplantation (David Type-1) group or a remodelling (Yacoub) group.

The details of the surgical and anaesthetic procedures prior to the surgical aortic root intervention have been described previously [14–16]. Following institution of extracorporeal circulation and cardioplegic arrest, the aortic valve was exposed through a transverse aortotomy 1 cm downstream from the commissures. For the surgical intervention groups, the ascending aorta was excised down to the aortic valve and replaced with a straight Dacron graft (22 mm Gelweave, Vascutek Ltd, Renfrewshire, UK). For the David Type-1 group (henceforth referred to as David), the aortic sinuses were also excised along with the coronary arteries. Next, the valve and coronary arteries were reimplanted into the straight Dacron graft. For the Yacoub procedure, the straight graft was tailored to match the curvature of aortic valve and sinuses. Hereafter, the graft was implanted to just above the aortic valve. Both techniques were performed as originally described by David and Yacoub [7, 8]. In the native group, no Dacron graft was implanted; however, a transverse aortotomy was performed to allow for implantation of force transducers and sonomicrometry crystals. The aorta was hereafter closed with Prolene 4-0 using a 2-layer technique with deep mattress sutures and a superficial over-and-over suture. Common to all groups was the implantation of 2 force transducers and 11 sonomicrometry crystals. Furthermore, mikro-tip<sup>®</sup> pressure catheters were inserted into the left ventricle and aortic arches.

The aortic root forces were measured with 2 force transducers [17]: the annulus transducer and the STJ transducer as depicted in Fig. 1. The annular transducer was inserted through an apical incision and fastened at the annular level with each force-sensing element sutured to the inter-leaflet triangles of the aortic valve and tightened using tourniquets on the outside of the aorta. Nine sonomicrometry crystals (1 and 2 mm, Sonometrics Corp., London, Canada) were placed throughout the aortic valve and root as illustrated in Fig. 2.

Three of these sonomicrometry crystals were inserted through the apical incision secured to the aortic annulus using non-elastic sutures (PremiCron 2-0, B. Braun, Melsungen, Germany), and 1 additional crystal was placed in the apex of the left ventricle for reference. In the aorta, 3 crystals were implanted at the commissures and 1 crystal on each mid-leaflet free edge. Hereafter, the STJ transducer was anchored around the aorta, with the force-sensing elements fastened to the commissures using tourniquets. Moreover, prior to aortic closure, a second reference crystal was placed in the aortic arch. After reperfusion, weaning off bypass and haemodynamic stabilization, force and haemodynamic data were acquired.

### Data acquisition and analysis

Data were collected in 2 sequences: the first dataset with the force transducers implanted and a second dataset with the force transducers removed. Approximately, 20 s of data was recorded during each acquisition sequence and stored for post-processing.

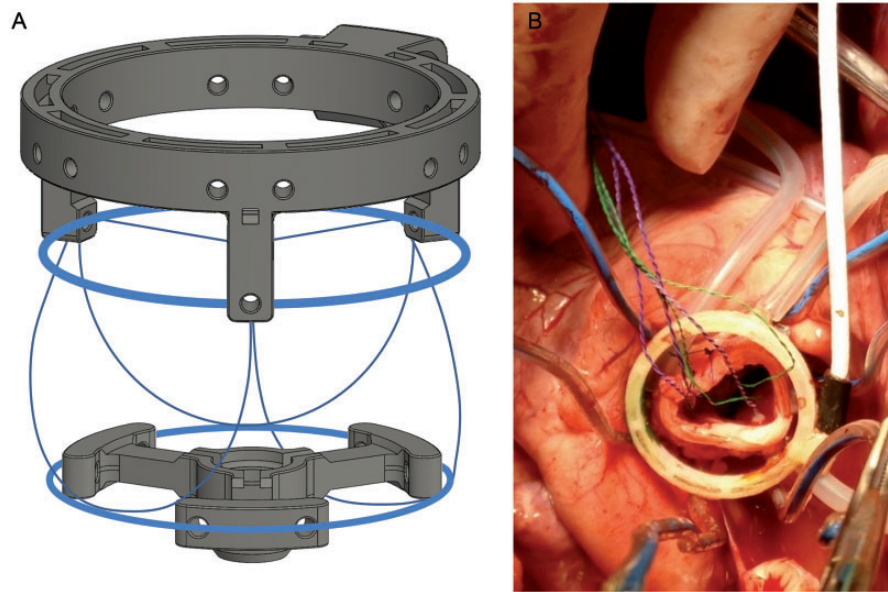


**Figure 1:** Force measurements. (A) Aortic root schematic with attached force transducers. (B) The sinotubular junction transducer being implanted on the native ascending aorta.

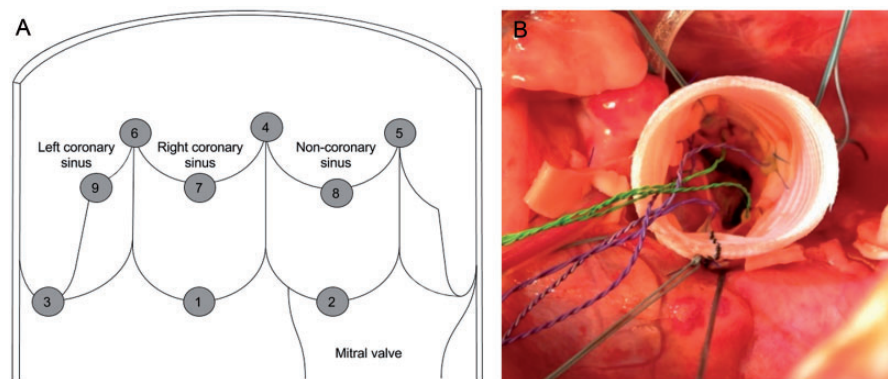


**Figure 2:** Geometrical changes. (A) Placement of the sonomicrometry crystals within the aortic root and (B) *in vivo* image from the ascending aorta displaying 1-mm cusp crystals (green wire) and 2-mm commissural crystals (purple wire).

For the second data acquisition, the tourniquets securing the force transducers were loosened, and both transducers were removed during beating heart under a short period of extracorporeal bypass. The annular transducer was pulled into the ventricle, and the STJ transducer was pulled towards the aortic arch.

The electrocardiogram (ECG) was amplified using a cardiomed system (Model 4008, CardioMed A/S, Oslo, Norway). The blood pressure was measured using mikro-tip catheters together with a signal conditioner (SPR-350 & PCU-2000, Millar Instruments, Houston, TX, USA). The analogue data (pressure, force and ECG) were all acquired with a sample rate of 1613 Hz using dedicated hardware and software (NI cDAQ 9172, NI 9237, NI 9215 and LabVIEW 2014, National Instruments, Austin, TX, USA). The sonomicrometry data were acquired at a sample rate of 297 Hz using the Sonometrics TRX USB system and the SonoLabDS3 software package (Sonometrics Corp.).

During the post-processing procedure, a 40-Hz second-order low-pass filter with a zero-phase response was applied on all data, from which 10 consecutive heart cycles were extracted.

The sonomicrometry data were post-processed using a commercial software package (SonoSoft v.3.4.71, Sonometrics Corp.),

and each crystal was represented by a 3-dimensional Cartesian coordinate set. The distances between 2 crystals were calculated as the Euclidian distance. From these data, 3 circular sectors [corresponding to the right-left (RL), right-non (RN) and left-non-coronary (LN) segment] were calculated for both the annular level and the STJ level. The geometric opening area was calculated as the area of the circumscribed circle of the triangle defined by the 3 leaflet crystals.

The reported force and geometry data were calculated as cyclic data by subtracting the minimum value from the maximum value for each segment. The time from the first time derivative of the ventricular pressure to the first time derivative of the geometric opening area ( $dP_{ventricle}/dt_{max}$  to  $d(\text{geometric opening area})/dt_{max}$ ) was defined as a measure of leaflet opening delay.

### Excluded data

Missing force data (due to strain gauge failure) were imputed based on the mean values from the same segment from all the other animals within the same group. Missing geometric data

(due to inadequate signal quality to obtain cyclic signal or dislocation of a sonomicrometry crystal) were imputed under the assumption of an equilateral triangle. Hence, the missing data were imputed based on the distance between the other 2 crystals within the same level.

## Statistical analysis

The sample size calculation (Equation 1) was based on force data from prior work performed by our group. We hypothesized that the forces would be significantly lower for both the David and Yacoub groups than for the native group.

$$n = 2 \left( (z\alpha + z\beta) \cdot \frac{\sigma}{\delta} \right)^2, \quad (1)$$

where  $n$  is the sample size,  $z\alpha$  and  $z\beta$  are the values of the 2-tailed  $z$ -distribution,  $\sigma$  is an estimate of the standard deviation, and  $\delta$  is the effect size. On the assumption of a standard deviation on annular forces of no more than 30%, a force reduction of 40% would be detected with a probability of 80% and  $\alpha$ -error 0.05 resulted in 7 animals per group and a total of 21 animals. Data are reported as mean  $\pm$  standard deviation. The extracted data were analysed using a mixed model with nested random

effects to account for the repeated measurements on animals and anatomical location within animals. Following the mixed model, residuals were inspected for normality, and no reason to refute this was found. Cross-clamp time and apparent root compliance were analysed using a One-way analysis of variance with a Bonferroni *post hoc* test. A  $P$ -value  $< 0.05$  was defined as a statistically significant difference. Stata 13.0 (StataCorp LLC, TX, USA) was used.

## RESULTS

Twenty-eight pigs were randomized into 3 groups, 22 of which were included in the study (native  $n = 7$ , David  $n = 7$  and Yacoub  $n = 8$ ). As the excluded animals provided no useable data, we compensated for this by including 7 additional pigs to the study.

Mean bodyweights of the pigs were  $80.9 \pm 2.6$  kg in the native group,  $81.0 \pm 3.0$  kg in the David group and  $80.1 \pm 1.5$  kg in the Yacoub group ( $P > 0.913$ ). Three pigs were excluded as they could not be weaned from the extracorporeal circulation, 2 were excluded due to malfunction of force transducers, and 1 pig died of uncontrollable cava vein bleeding. One animal was excluded from the David group, 2 from the Yacoub group and 3 from the native group.

**Table 1:** Haemodynamic parameters for all included animals

	Dataset 1: with force measurements, mean $\pm$ SD			Dataset 2: without force measurements, mean $\pm$ SD		
	Native ( $n = 7$ )	David ( $n = 7$ )	Yacoub ( $n = 8$ )	Native ( $n = 7$ )	David ( $n = 7$ )	Yacoub ( $n = 8$ )
HR (BPM)	108 $\pm$ 28	131 $\pm$ 17	132 $\pm$ 30	120 $\pm$ 15	132 $\pm$ 20	152 $\pm$ 24
$dP/dt_{\max}$ (mmHg/s)	1672 $\pm$ 422	1563 $\pm$ 578	1389 $\pm$ 469	1859 $\pm$ 531	1625 $\pm$ 689	1442 $\pm$ 467
LVP <sub>max</sub> (mmHg)	93 $\pm$ 11	93 $\pm$ 21	84 $\pm$ 19	96 $\pm$ 25	90 $\pm$ 22	79 $\pm$ 17
AP <sub>max</sub> (mmHg)	62 $\pm$ 15	61 $\pm$ 10	63 $\pm$ 11	71 $\pm$ 26	63 $\pm$ 12	61 $\pm$ 13
TvP <sub>max</sub> (mmHg)	36 $\pm$ 12	42 $\pm$ 9	24 $\pm$ 15	29 $\pm$ 20	41 $\pm$ 18	21 $\pm$ 11

AP<sub>max</sub>: maximum aortic pressure;  $dP/dt_{\max}$ : maximum rate of change of left ventricular pressure; HR: heart rate; LVP<sub>max</sub>: maximum left ventricular pressure; TvP<sub>max</sub>: maximum transvalvular pressure.

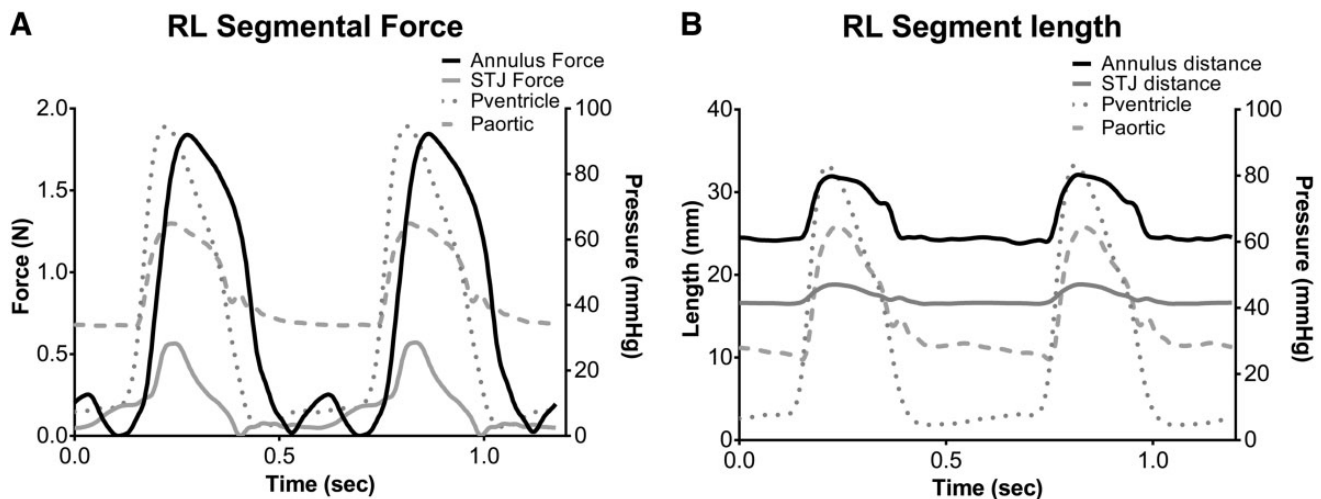


**Figure 3:** Data example from the RL segment in a native pig. (A) The annular and sinotubular junction forces. (B) The circular segment lengths for the annulus and sinotubular junction. In both graphs, the ventricular and aortic pressures are plotted for reference. R-L: right-left; STJ: sinotubular junction.

Cross-clamp times for the groups were  $81 \pm 13$  min in the native group,  $116 \pm 26$  min in the David group and  $110 \pm 12$  min in the Yacoub group, with the time in the native group being significantly shorter than in the intervention groups ( $P = 0.005$ ).

Within the annular level, the radii of the circumscribed circle were  $12.1 \pm 0.8$  mm in the native group,  $11.4 \pm 0.6$  mm in the David group and  $11.7 \pm 0.8$  mm in the Yacoub group ( $P > 0.118$ ). At the STJ level, the radii were  $9.2 \pm 0.8$  mm in the native group,  $7.9 \pm 0.9$  mm in the David group and  $8.9 \pm 1.0$  mm in the Yacoub group ( $P > 0.051$ , while native to David  $P = 0.015$ ).

Sixty-six geometric and force segments were defined at the annular level and 66 at the STJ level, yielding a total of 132. In the geometric dataset, 11 annular (LR = 4, LN = 4 and RN = 3) and 6 STJ (LR = 3, LN = 1 and RL = 2) segments were imputed. In the force datasets, eight annular (LR = 1, LN = 2 and RN = 5) and no STJ segments were imputed. The force and geometry data were collected during haemodynamic conditions, as listed in Table 1, with and without force measurements. A representative example of both force and geometry data from the right-left segment in a native pig are shown in Fig. 3.

The heart rate was statistically significantly different between the native and Yacoub groups in the *without force* dataset ( $P = 0.013$ ). In both datasets, there was a statistical difference in

the transvalvular pressure between the David and Yacoub groups ( $P < 0.039$ ).

At the annular level, the RL segment displays the highest force amplitudes in all groups (Fig. 4A). Within the native group, the force in the RL segment was higher than in the other 2 segments ( $P = 0.025$ ).

Furthermore, within the Yacoub group, the annular force was lowest in the LN segment compared with the other 2 segments ( $P < 0.001$ ), while annular forces were not statistically different within the David group.

Segmental forces in the STJ were significantly increased in the native group compared with the intervention groups (Fig. 4B) with the exception of the RL segment between the native and the Yacoub groups ( $P = 0.586$ ). No statistical difference between the 3 segments within a single group was found, except for the Yacoub group. Here, the LN cyclic force was decreased compared with the other segments ( $P < 0.004$ ). Furthermore, the cyclic force amplitude in the 2 intervention groups was not different ( $P = 0.123$ ).

At the annular level, the cyclic length of the LN segment in the native group was larger ( $P = 0.007$ ) than in the intervention groups (Fig. 5A). Within the Yacoub group, the LN segment was shorter than the other segments ( $P = 0.024$ ). Within the native group, the RL segment was shorter than the other segments

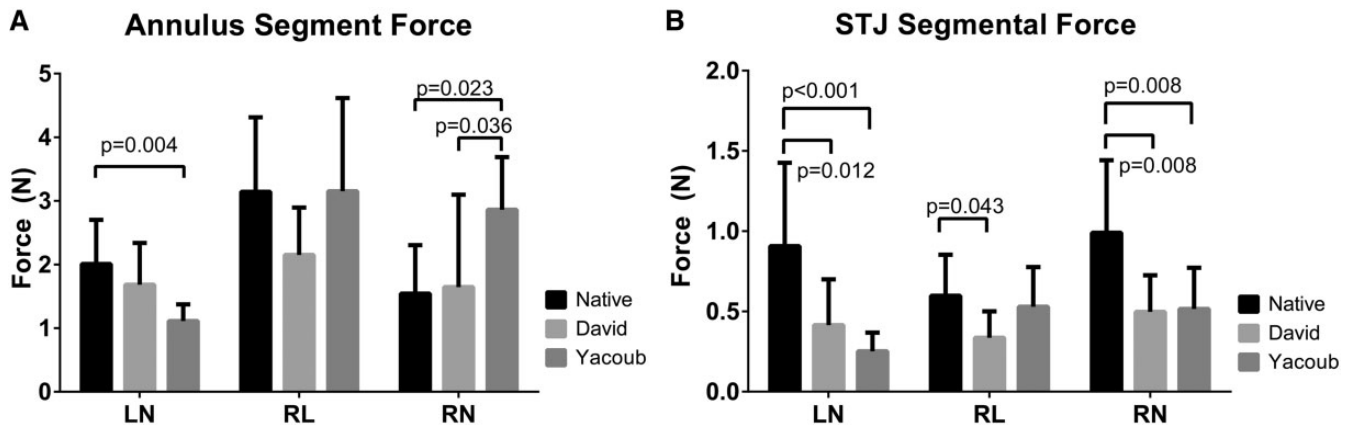


Figure 4: Segmental forces of the (A) aortic annulus and (B) the STJ. LN: left-non-coronary; RL: right-left coronary; RN: right-non-coronary; STJ: sinotubular junction.

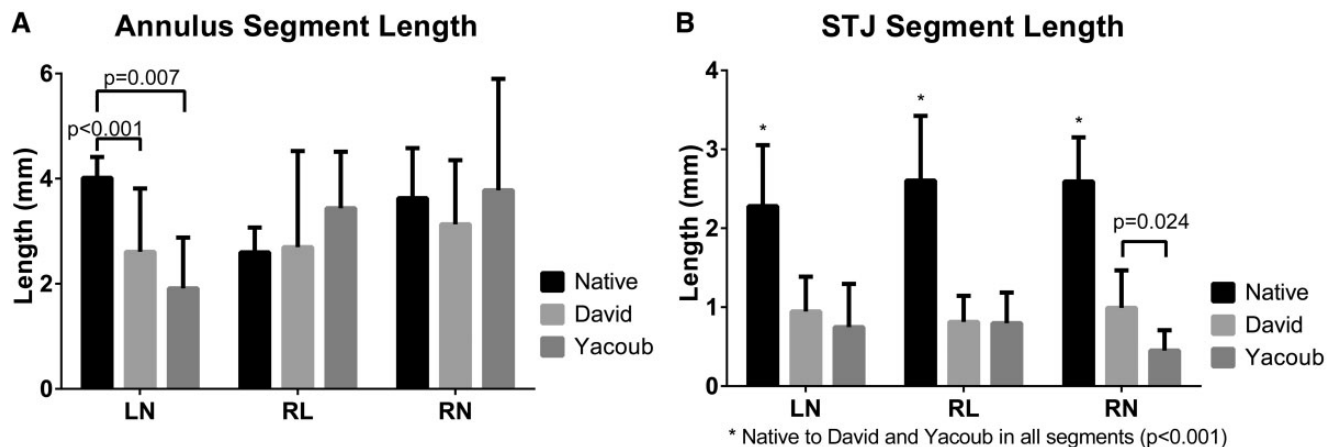
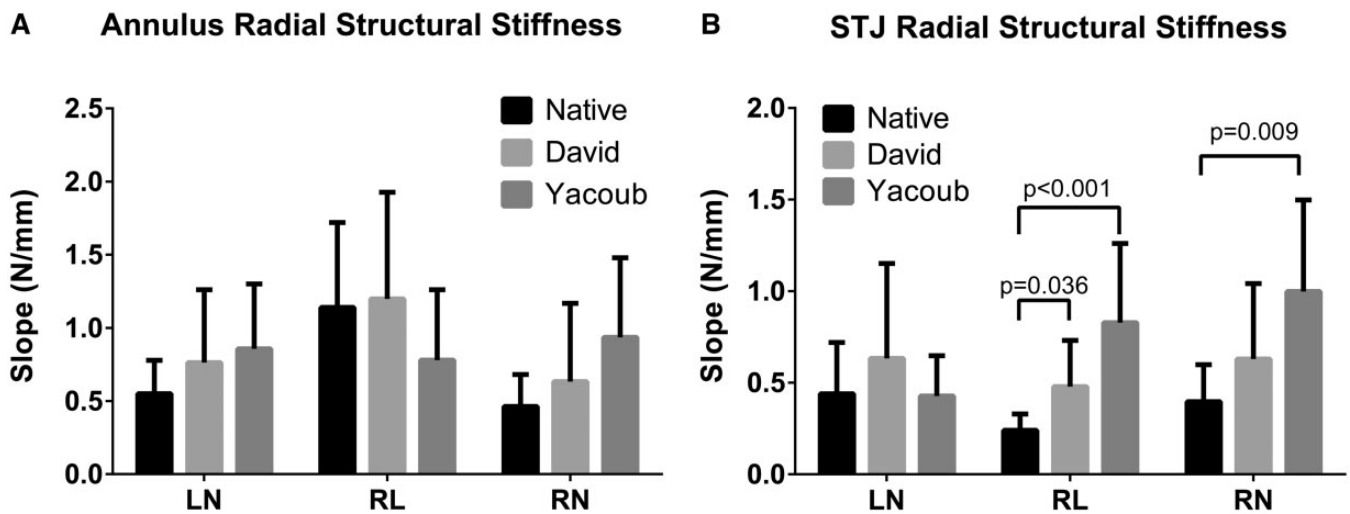


Figure 5: Segmental length for the (A) aorta annulus and (B) the STJ. LN: left-non-coronary; RL: right-left coronary; RN: right-non-coronary; STJ: sinotubular junction. \*Native to David and Yacoub in all segments ( $P < 0.001$ ).



**Figure 6:** Radial structural stiffness for the individual segments of the (A) aortic annulus and (B) the STJ. LN: left-non-coronary; RL: right-left coronary; RN: right-non-coronary; STJ: sinotubular junction.

( $P=0.002$ ). No difference between the segments within the David group was found ( $P=0.527$ ).

In the STJ (Fig. 5B), the cyclic length was larger in all segments in the native group compared with both interventions. The RN segment in the Yacoub group had a significantly smaller cyclic length than in David group. Within the Yacoub group, the RN segment was also significantly smaller than the LN segment ( $P=0.038$ ).

None of the radial structural stiffnesses between groups at the annular level (Fig. 6A) was statistically different ( $P>0.064$ ). Within the native group, the RL segment was stiffer than the other 2 segments ( $P=0.007$ ). Within the David group, the RL segment was stiffer than the RN ( $P=0.029$ ) but not the LN segment ( $P=0.092$ ). No difference was found within the Yacoub group ( $P=0.435$ ).

At the STJ (Fig. 6B), the RL and RN segments were less compliant in the Yacoub group than the other groups. Furthermore, within the Yacoub group, the LN segment was more compliant than both the RL and RN segments ( $P=0.025$ ). No segments were different within the David group ( $P=0.335$ ) or the native group ( $P=0.090$ ).

The elastic energy stored within the aortic root was  $882 \pm 552 \mu\text{J}$  in the native group,  $886 \pm 344 \mu\text{J}$  in David group and  $431 \pm 184 \mu\text{J}$  in the Yacoub group. There was no difference between the David and native ( $P=0.990$ ) groups or the David and Yacoub ( $P=0.051$ ) groups, but the Yacoub group had significantly lower elastic energy stored than the native group ( $P=0.041$ ).

The geometric opening area was  $358 \pm 60 \text{ mm}^2$  in the native group,  $204 \pm 75 \text{ mm}^2$  in the David group and  $236 \pm 58 \text{ mm}^2$  in the Yacoub group. The native group had the largest geometric opening area compared with both interventions ( $P<0.001$ ), and the Yacoub group was larger than the David group ( $P=0.030$ ).

The leaflet opening delay was  $21.6 \pm 9.1 \text{ ms}$  in the native group,  $24.7 \pm 19.7 \text{ ms}$  in the David group and  $21.3 \pm 18.6 \text{ ms}$  in the Yacoub group, and thus there was no difference between groups ( $P=0.309$ ).

## DISCUSSION

In this study, we combine several measurement techniques to describe the biomechanical differences between the native aortic root and 2 original valve-sparing interventions. This study is the

first to combine force data with geometrical data to obtain the radial structural stiffness of different segments in both native and repaired aortic roots.

In our study, the native and David groups showed similar force patterns at the annular level, while force development in the Yacoub group was different and statistically greater in the RN segment than in the other groups.

In the RL segment, which correlates with the muscular portion of the annulus [18], the forces in the Yacoub and native groups were almost identically, while the force in the David group was about 30% lower. This can be explained by the difference in graft design between the 2 interventions, where the David procedure offers the greatest annular stabilization, resulting in a lower measured force.

The geometry at the annular level has been reported as changing from ellipsoid in diastole to a more round configuration during systole [19, 20], which can explain the difference in cyclic segment length in our study. Furthermore, small variations within segments can be due to a minor change in the principal direction of this ellipsoid configuration between groups. In the 2 intervention groups, this shift in the principal axis was most likely caused by a difference in the design of the graft, and hereby the degree of stabilization in the grafts in the intervention groups. In the David group, the cycle length appeared to be maintained at the same level between segments. This is also supported by the force measurements in the David group, where the 3 annular segments are similar in amplitude, suggesting stabilization and averaging-out of forces. The cyclic length of the annular RL segment is minimized by the contraction of the muscular portion, which furthermore can explain the relatively large force within this segment.

The forces within all 3 segments of the STJ were similar in the 2 intervention groups, and they were significantly lower than the forces in the native group. This is because both interventions are stabilized at the STJ by the tubular graft. This graft absorbed the dilatation forces, which were primarily due to blood being ejected from the ventricle during systole.

In the native group, the forces within the STJ seem to be largest in the segments containing the non-coronary cusp. The same segment has been reported to be more prone to degeneration [21], which may explain the larger force within this segment.

The segmental dilatation in the native group seems more uniform in the STJ, which indicates a circular geometry in both systole and diastole. The same pattern can be seen in the 2 intervention groups, where the cyclic lengths in all segments were statistically smaller than in the native group. This limited distention is a result of an equal stabilization of the STJ in both procedures as the graft design is comparable at this level. Hence, both segmental force and segmental length are expected to be similar between the interventions at this level.

In all groups, the least compliant annular segment seemed to be the RL segment, which is in agreement with the previous discussion regarding muscular contraction and segment shortening. The exception was the RL segment within the Yacoub group, which appeared to be the most compliant segment, although the differences between groups were non-significant ( $P > 0.435$ ). This could be explained by an equalization of tension in the 3 segments due to the semistabilizing design of the Yacoub graft, which might dissipate tension in an equal manner. This could be a positive indicator with regard to the longevity of the Yacoub root repair.

The Yacoub procedure seems less dynamic than the other groups with regard to measures of radial structural stiffness and elastic energy storage in the aortic root even though it has been reported to preserve annular distensibility [5, 22]. It is plausible that the Yacoub procedure diverts the root dilation towards the sinuses, but since no sonomicrometry crystals were implanted in the sinuses this theory could not be tested. However, in both the Yacoub and native groups the geometric opening area was markedly larger than in the David group. This supports the theory, and this can be explained by the Yacoub procedure maintaining the sinuses of Valsalva, which are reported to facilitate near-normal cusp dynamics [10, 23, 24]. Furthermore, the transvalvular pressure was larger in the David group than in the 2 other groups, which also correlates with the lower geometric opening area.

Judging from the transvalvular pressures, one can speculate that a Dacron size of 22 mm was too small; however, no statistical difference was found in the annular radii within the 3 groups. Furthermore, a 'one-size-fits-all' technique was deployed, since the pigs included had very similar bodyweights and also a similar aorta size. This was matched with the force transducers, which were only available in 1 size. Nevertheless, increasing the Dacron size might lower the transvalvular pressure in the 2 groups.

At both the annular and STJ levels, the native group tended to be the most flexible group. An obvious explanation is the lack of a supporting graft in the native group. In both intervention groups, the mechanical properties of the aortic root were changed due to the graft design, which could be the reason for different stiffness measurements in these 2 groups. Based on the current study, it seems that patients with a dilated aortic root, secondary to a connective tissue disorder, may benefit from the annular stabilization afforded by the David procedure, which would inhibit later annular redilatation. If the aortic root repair is required due to factors other than connective tissue disorders, the patient may benefit from receiving the Yacoub procedure in order to maintain the valve dynamics.

## Limitations

The cross-clamp time was significantly different in the native group compared with the other interventions, which could skew some

results. Furthermore, the force and geometry dataset were collected with a minor time delay between them, during which the cardiac dynamics could have changed. However, there was no difference in the derivative of left ventricular pressure, indicating that the contractility of the heart was equal in all groups. Missing data were imputed, which may skew the results and produce smaller than actual deviations; however, discarding entire datasets would result in an underpowered study. As the force-sensing elements are not completely perpendicular to each other, crosstalk will be introduced in the opposite sensing arms of the annular force transducer, which will result in an overestimation of the force amplitude. To avoid aortic root pathology influencing the results of this study, only healthy pigs were used. This ensures that the actual biomechanical differences measured are on the basis of the different interventions only; nonetheless, this makes it difficult to translate our results directly to the clinical setting.

## CONCLUSION

In general, the native group in our study had the largest force amplitude and the largest cyclic geometrical change compared with the 2 intervention groups. The overall force was lowest in the David group, indicating the most pronounced stabilization within this group. The cyclic geometrical changes were comparable within the 2 intervention groups; however, the Yacoub procedure offered a larger geometric opening area than the David procedure, facilitating less flow resistance in the aortic root and hence a lower transvalvular pressure. No major differences were observed between the animals in the David and Yacoub groups.

## Funding

This work was supported by the Danish Heart Foundation Grant [15-R99-A5942-22906, 13-04-R94-A4620-22804], the Danish Council for Independent Research Grant [DFF-4004-00317], Aarhus University, Direktør Jacob Madsens & Hustru Olga Madsens Fond, Direktør Kurt Bønnelycke og hustru fru Grethe Bønnelyckes Fond, Edith og Olfert Dines Hansens Legat, Helga og Peter Kornings fond, Holger Rabitz og hustru Doris Mary født Philipp's Mindefond, Snedkermester Sophus Jacobsen og hustru Astrid Jacobsens Fond and Karen Elise Jensens Fond.

**Conflict of interest:** none declared.

## REFERENCES

- [1] Bentall H, De Bono A. A technique for complete replacement of the ascending aorta. *Thorax* 1968;23:338-9.
- [2] Moodie DS. Replacement of the aortic root in patients with Marfan syndrome. *Clin Pediatr (Phila)* 2000;39:683.
- [3] Nezafati P, Shomali A, Nezafati MH. A simple modified Bentall technique for surgical reconstruction of the aortic root—short and long term outcomes. *J Cardiothorac Surg* 2015;10:1-7.
- [4] Hirasawa Y, Aomi S, Saito S, Kihara S, Tomioka H, Kurosawa H. Long-term results of modified Bentall procedure using flanged composite aortic prosthesis and separately interposed coronary graft technique. *Interact CardioVasc Thorac Surg* 2006;5:574-7.
- [5] Erasmi AW, Sievers H-H, Bechtel JF, Hanke T, Stierle U, Misfeld M. Remodeling or reimplantation for valve-sparing aortic root surgery? *Ann Thorac Surg* 2007;83:S752-6; discussion S785-90.

- [6] Johansen P, Hansen SB, Hasenkam JM, Nygaard H. Noise levels of closing sounds in vivo are equal for different bileaflet mechanical heart valves. *J Heart Valve Dis* 2003;12:764–71.
- [7] David TE, Feindel CM. An aortic-valve sparing operation for patients with aortic incompetence and aneurysm of the ascending aorta. *J Thorac Cardiovasc Surg* 1992;103:617–22.
- [8] Sarsam MA, Yacoub M. Remodeling of the aortic-valve annulus. *J Thorac Cardiovasc Surg* 1993;105:435–8.
- [9] Shimizu H, Yozu R. Valve-sparing aortic root replacement. *Ann Thorac Cardiovasc Surg* 2011;17:330–6.
- [10] David TE. Aortic valve sparing operations: a review. *Korean J Thorac Cardiovasc Surg* 2012;45:205–12.
- [11] Dagum P, Green GR, Nistal FJ, Daughters GT, Timek TA, Foppiano LE *et al.* Deformational dynamics of the aortic root: modes and physiologic determinants. *Circulation* 1999;100:1154–62.
- [12] Cheng A, Dagum P, Miller DC. Aortic root dynamics and surgery: from craft to science. *Philos Trans R Soc Lond B Biol Sci* 2007;362:1407–19.
- [13] Lansac E, Lim HS, Shomura Y, Lim KH, Rice NT, Goetz W *et al.* A four-dimensional study of the aortic root dynamics. *Eur J Cardiothorac Surg* 2002;22:497–503.
- [14] Hasenkam JM, Nygaard H, Paulsen PK, Kim WY, Hansen OK. What force can the myocardium generate on a prosthetic mitral valve ring? An animal experimental study. *J Heart Valve Dis* 1994;3:324–9.
- [15] Nielsen SL, Lomholt M, Johansen P, Hansen SB, Andersen NT, Hasenkam JM. Mitral ring annuloplasty relieves tension of the secondary but not primary chordae tendineae in the anterior mitral leaflet. *J Thorac Cardiovasc Surg* 2011;141:732–7.
- [16] Jensen MØ, Jensen H, Nielsen SL, Smerup M, Johansen P, Yoganathan AP *et al.* What forces act on a flat rigid mitral annuloplasty ring? *J Heart Valve Dis* 2008;17:267–75; discussion 275.
- [17] Bechsgaard T, Hønge JL, Nygaard H, Nielsen SL, Johansen P. Biomechanical assessment of the aortic root using novel force transducers. *J Biomech* 2017;61:58–64.
- [18] Komiya T. Aortic valve repair update. *Gen Thorac Cardiovasc Surg* 2015;63:309–19.
- [19] de Heer LM, Budde RP, Mali WP, de Vos AM, van Herwerden LA, Kluijn J. Aortic root dimension changes during systole and diastole: evaluation with ECG-gated multidetector row computed tomography. *Int J Cardiovasc Imaging* 2011;27:1195–204.
- [20] Suchá D, Tuncay V, Prakken NH, Leiner T, Van Ooijen PM, Oudkerk M. Does the aortic annulus undergo conformational change throughout the cardiac cycle? A systematic review. *Eur Heart J Cardiovasc Imaging* 2015;16:1307–17.
- [21] Cotrufo M, De Santo LS, Esposito S, Renzulli A, Della Corte A, De Feo M *et al.* Asymmetric medial degeneration of the ascending aorta in aortic valve disease: a pilot study of surgical management. *J Heart Valve Dis* 2001;81:37–41.
- [22] Leopaldi AM, Vismara R, Lemma M, Valerio L, Cervo M, Mangini A *et al.* *In vitro* hemodynamics and valve imaging in passive beating hearts. *J Biomech* 2012;45:1133–9.
- [23] Katayama S, Umetani N, Sugiura S, Hisada T. The sinus of Valsalva relieves abnormal stress on aortic valve leaflets by facilitating smooth closure. *J Thorac Cardiovasc Surg* 2008;136:1528–35, 1535.e1.
- [24] Leyh RG, Schmidtke C, Sievers H-H, Yacoub MH. Opening and closing characteristics of the aortic valve after different types of valve-preserving surgery. *Circulation* 1999;100:2153–60.